WATER RESOURCES RESEARCH, VOL. 24, NO. 7, PAGES 1048–1060, JULY 1988

A Distributed Parameter Approach for Evaluating the Accuracy of Groundwater Model Predictions 2. Application to Groundwater Flow

DENNIS MCLAUGHLIN

Ralph M. Parsons Laboratory, Department of Civil Engineering, Massachusetts Institute of Technology, Cambridge

ERIC F. WOOD

Water Resources Program, Department of Civil Engineering, Princeton University, Princeton, New Jersey

The distributed parameter theory presented by McLaughlin and Wood (this issue) is used to evaluate the accuracy of a groundwater flow model. The special case investigated assumes that the model's prediction errors are due primarily to data limitations. In this case, approximate prediction error moments (mean and covariance) are obtained by solving two sets of coupled partial differential equations which have the same basic structure as the original flow equation. Solutions can be obtained with spectral, Green's function, or numerical techniques, depending on the assumptions made. Two examples are solved using a finite element approach. The first (two-dimensional) example confirms steady state infinite domain results obtained with spectral methods. The second (three-dimensional) example investigates the influence of spatial variability, sampling strategy, and suboptimal estimation on model prediction accuracy.

INTRODUCTION

It is generally recognized that a groundwater model's accuracy is strongly dependent on the quantity and quality of data used to estimate its inputs and on the heterogeneity of the natural system that it attempts to describe. Until recently, however, the connections between accuracy, data, and heterogeneity were not well understood, and there were no clear guidelines for evaluating the likely performance of models designed to predict environmental impacts. The stochastic approach to groundwater hydrology has provided new analytical techniques which shed light on the many factors affecting prediction accuracy. Contributions in this area have been made by many investigators, including *Freeze* [1975], *Tang and Pinder* [1979], *Sagar* [1978], *Cooley* [1977, 1979], *Smith and Freeze* [1979*a*, *b*], *Dettinger and Wilson* [1981], *Yeh and Yoon* [1981], *Dagan* [1982*a*, *b*], *Clifton and Neuman* [1982], *Townley* [1983], *Hoeksema and Kitanidis* [1984], *Carrera and Neuman* [1986], *Gelhar* [1986], and *Chu et al.* [1987]. In a companion paper [*McLaughlin and Wood*, this issue] we present a stochastic approach to accuracy evaluation which is based on distributed parameter estimation theory. This approach explicitly considers the combined effects of spatial variability, sampling strategy, input estimation, and model approximations. It provides a way to assess the accuracy of model predictions before they are used to make expensive or irreversible management decisions.

In this paper, we describe an application of our accuracy analysis procedure to a relatively simple groundwater flow problem: prediction of the drawdown in a spatially heterogeneous confined aquifer. Drawdown predictions are derived from a discretized and spatially aggregated model of the "real world," which is described by a set of stochastic "reference equations." The model's inputs are assumed to be estimated from a small number of noisy field observations. Model accuracy is measured in terms of the prediction error, which is simply the difference between the reference and predicted heads. We are particularly interested in the way modeling decisions can affect the mean and variance of this error.

The general theory presented by *McLaughlin and Wood* [this issue] is designed to examine the effects of errors in model structure as well as those related to sampling and input estimation. The accuracy analysis can, however, be greatly simplified if structural and discretization errors are neglected. In this special case many of the moment equations included in the general formulation can be dropped, and the computational effort needed to solve problems of realistic size decreases significantly. Of course, structural errors can have a significant effect on prediction accuracy, particularly when basic model assumptions (such as vertical homogeneity) are invalid or when the model's boundary conditions are inappropriate. For present purposes, however, we focus on applications where the model is properly formulated and prediction error is due primarily to data limitations.

The next section of this paper presents the state and moment equations used in our groundwater flow analysis. This is followed by a review of methods for solving the moment equations and a discussion of two numerical examples. The paper concludes with some observations on other applications of the general approach.

PROBLEM FORMULATION

The distributed groundwater system which is used as a reference for our accuracy analysis is described by the following time-dependent saturated flow equation:

$$s\frac{\partial y}{\partial t} = \nabla \cdot [e^{g}\nabla y] + q \qquad \mathbf{r} \in D \tag{1a}$$

$$y = y_b \qquad \mathbf{r} \in \partial D_1 \tag{1b}$$

$$\nabla y \cdot \mathbf{n} = 0 \qquad \mathbf{r} \in \partial D_2 \tag{1c}$$

$$y = y_0 \qquad \mathbf{r} \in D \qquad t = t_0 \tag{1d}$$

Paper number 7W4979.
0043-1397/88/007W-4979$05.00

The dependent variable $y(\mathbf{r}, t)$ is the hydraulic head or drawdown defined at time t and location $\mathbf{r}$ over a confined two- or three-dimensional region D with boundary ∂D. The forcing term $q(\mathbf{r}, t)$ is the net inflow rate from external sources and $y_0(\mathbf{r})$ is a specified initial condition. A specified time-invariant head boundary condition $y_b(\mathbf{r})$ is imposed over part of the boundary (∂D_1), while a zero flux condition is imposed over the remainder (∂D_2). The vector $n(\mathbf{r})$ is the outward pointing unit vector normal to ∂D_2 at the point $\mathbf{r}$. If D is two-dimensional, $\theta(\mathbf{r})$ is the log transmissivity, s is a spatially invariant storage coefficient, and y is understood to be vertically averaged. If D is three-dimensional, $\theta(\mathbf{r})$ is the log hydraulic conductivity and s is a spatially invariant specific storage parameter. Log transmissivity and conductivity parameters are used primarily because they tend to be normally distributed and yield reasonably robust first- and second-order approximations [*Freeze*, 1975; *Gutjahr*, 1984]. The log transformation is, however, not essential.

The examples presented later in this paper are concerned with the effects of spatial heterogeneity on prediction accuracy. Stochastic methods provide a convenient way to describe heterogeneity, particularly when field measurements can be used to estimate the ensemble statistics of the reference inputs. Here we focus on heterogeneities in the log hydraulic conductivity distribution, which is assumed to behave as if it were a sample function drawn from a random population with a known mean and covariance. All other reference inputs, such as the storage coefficient, source rate, and auxiliary conditions, are known deterministic quantities. This restriction can be relaxed if the definition of θ is expanded to include other sources of uncertainty [*McLaughlin and Wood*, this issue].

We assume that the groundwater flow model used to predict the reference state is derived by discretizing a deterministic version of (1) over the region D. That is, there are no "structural" differences between the model and reference system. We also assume that the computational grid is fine enough to insure that discretization errors can be neglected. As mentioned earlier, these two assumptions greatly simplify the prediction error moment equations and allow us to concentrate on sampling and input estimation questions [*McLaughlin*, 1985; *McLaughlin and Wood*, this issue]. The discretized model equation corresponding to (1) has the following general form [*Pinder and Gray*, 1977]:

$$C(S)\frac{dY(t)}{dt} = A(\Theta)Y + B(Q, Y_b) \tag{2a}$$

$$Y = Y_0 \qquad t = t_0 \tag{2b}$$

$$\hat{y}(\mathbf{r}, t) = \phi(\mathbf{r})^T Y(t) \tag{2c}$$

where the dependent variable $Y(t)$ is a vector of M hydraulic heads or drawdowns defined at the nodes of the computational grid. The vector $\phi(\mathbf{r})$ is composed of interpolation functions which are used to derive model predictions at locations between grid nodes (a superscript T indicates vector or matrix transposition). If the model is two-dimensional, Θ is a vector of discretized log transmissivities, S is a vector of discretized storage coefficients, and Y is understood to be vertically averaged. If it is three-dimensional, Θ is a vector of discretized log hydraulic conductivities and S is a vector of discretized specific storage parameters.

The model's other discretized inputs are the source rate vector Q, the initial head vector Y_0, and the vector of specified heads Y_b defined at nodes on the boundary surface ∂D_1. Zero normal fluxes are imposed at the boundary nodes on the boundary surface ∂D_2. For simplicity, we assume that all discretized inputs are specified at the nodes of the computational grid. Also, we assume that the elements of Θ are estimated from noisy measurements of θ but that all other inputs are known perfectly. This is consistent with our previous assumption that the reference storage coefficient, source rate, and auxiliary conditions are known deterministic variables.

The definitions of the M by M-dimensional matrix functions C and A and the M-dimensional vector function B depend on the particular discretization technique selected. If a Galerkin finite element procedure is used and the assumptions listed above are imposed, the scalar elements of C, A, and B have the following form [*Pinder and Gray*, 1977]:

$$C_{mn} = \int_D \{[\phi_k(\mathbf{r})S_k]\phi_m(\mathbf{r})\phi_n(\mathbf{r})\}\, d\mathbf{r} \qquad \mathbf{r}_m, \mathbf{r}_n \notin \partial D_1 \tag{3a}$$

$$C_{mn} = 0 \qquad \text{otherwise}$$

$$A_{mn} = -\int_D \{[\phi_k(\mathbf{r}) \exp(\Theta_k)][\nabla\phi_m(\mathbf{r}) \cdot \nabla\phi_n(\mathbf{r})]\}\, d\mathbf{r} \qquad \mathbf{r}_m \notin \partial D_1 \tag{3b}$$

$$A_{mn} = \delta_{mn} \qquad \mathbf{r}_m \in \partial D_1$$

$$B_m = -\int_D \{[\phi_k(\mathbf{r})Q_k(t)]\phi_m(\mathbf{r})\}\, d\mathbf{r} \qquad \mathbf{r}_m \notin \partial D_1 \tag{3c}$$

$$B_m = -Y_{bm} \qquad \mathbf{r}_m \in \partial D_1$$

where $\phi_k(\mathbf{r})$ is the interpolation function associated with node k, $\mathbf{r}_m$ is the location of node m, and δ_{mn} is one when $m = n$ and zero otherwise. All indices vary from 1 to M, with implied summation over repeated subscripts.

Now suppose that the uncertain model input vector Θ is estimated from N noisy point measurements of the reference input $\theta(\mathbf{r})$. The measurements could be obtained from soil samples, slug tests, or other sources, depending on the application. If the estimator is linear, the estimation equation for this simplified problem is given by (10*b*) of *McLaughlin and Wood* [this issue]:

$$\Theta = \Gamma + \Lambda Z \tag{4}$$

where Z is a measurement vector with components

$$[Z]_n = \theta(\mathbf{r}_n) + [\Omega]_n \tag{5}$$

Here $\mathbf{r}_n$ is the coordinate of the nth measurement and the measurement error vector Ω is assumed to be zero mean with a known covariance R. The M-dimensional vector Γ and the M by N-dimensional matrix Λ are weighting coefficients which depend on the particular linear estimator selected [*Kitanidis*, 1986]. We suppose that Θ is estimated with a conventional kriging algorithm which assumes that the covariances P_{ZZ} and $P_{Z\Theta}$ are known but that the mean $\bar{\Theta}$ is an unknown constant. In this case, the Γ vector is identically zero, and the elements of Λ are obtained by solving the following system of $M(N + 1)$ equations in $M(N + 1)$ unknowns [*Journel and Huijbreghts*, 1978]:

$$\Lambda_{ik}[\hat{P}_{ZZ}]_{kn} + \mu_i = [\hat{P}_{\Theta Z}]_{in} \qquad i = 1 \cdots M \quad n = 1 \cdots N \tag{6a}$$

$$\Lambda_{ik}u_k = 1 \qquad i = 1 \cdots M \tag{6b}$$

where k is summed from 1 to N, $u_k = 1$ for all k, and μ_i is an unknown Lagrange multiplier. The covariances $\hat{P}_{ZZ}$ and $\hat{P}_{\Theta Z}$

are the estimated covariances used to compute the weighting matrix Λ. The kriging algorithm will be suboptimal if these covariances are incorrect or if the mean of Θ is not actually constant.

The above equations provide all the information needed to compute model predictions from field observations. The resulting prediction error at any location $\mathbf{r}$ and time t is

$$\tilde{y}(\mathbf{r}, t) = y(\mathbf{r}, t) - \phi(\mathbf{r})^T Y(t) \tag{7}$$

Approximate expressions for the moments of this error and the related reference and model states are given by *McLaughlin and Wood* [this issue]. In order to use these expressions we need to identify the various derivatives which result when (1) and (2) are expanded to second order. The functional derivatives associated with (1) may be obtained by perturbing y and θ about their respective means, expanding, and collecting terms of like order. The resulting zero-, first-, and second-order terms are listed, using the notation of *McLaughlin and Wood* [this issue], in Table 1. The matrix derivatives associated with (2) may be obtained by differentiating (3) with respect to the appropriate scalar components of Θ and Y. The resulting terms are listed in Table 2.

We start by stating the equations for the reference and model moments, which are needed to obtain the moments of the prediction error. For simplicity, we assume that the reference log conductivity (or log transmissivity) is wide sense stationary. That is, it has a known constant mean $\bar{\theta}$ and a known covariance $P_{\theta\theta}(\mathbf{r} - \mathbf{r}')$ which depends only on the difference between the locations $\mathbf{r}$ and $\mathbf{r}'$. In this case, the following reference mean equation results when the derivative definitions of Table 1 are substituted into (14) of *McLaughlin and Wood* [this issue]:

$$\frac{s}{k_g}\frac{\partial \bar{y}}{\partial t} \simeq [1 + \tfrac{1}{2}\sigma_\theta{}^2]\nabla^2\bar{y} + \nabla \cdot [\nabla P_{y\theta}]_{\mathbf{r}'=\mathbf{r}} + \frac{q}{k_g} \qquad \mathbf{r} \in D \tag{8a}$$

$$\bar{y} = y_b \qquad \mathbf{r} \in \partial D_1 \tag{8b}$$

$$\nabla\bar{y} \cdot \mathbf{n} = 0 \qquad \mathbf{r} \in \partial D_2 \tag{8c}$$

$$\bar{y} = y_0 \qquad \mathbf{r} \in D \tag{8d}$$

TABLE 1. Reference System Operators for the Groundwater Flow Example

Operator	Definition
$f(y,\theta)$	$\frac{1}{s}\nabla \cdot [e^{\theta}\nabla y] + \frac{1}{s}q$
$f(\bar{y}, \bar{\theta})$	$\frac{1}{s}\nabla \cdot [k_g\nabla\bar{y}] + \frac{1}{s}q$
$f_y\delta y$	$\frac{1}{s}\nabla \cdot [k_g\nabla(\delta y)]$
$f_\theta\delta\theta$	$\frac{1}{s}\nabla \cdot [k_g(\delta\theta)\nabla\bar{y}]$
$f_{yy}\delta y\delta y$	0
$f_{y\theta}\delta y\delta\theta$	$\frac{1}{s}\nabla \cdot [k_g(\delta\theta)\nabla(\delta y)]$
$f_{\theta\theta}\delta\theta\delta\theta$	$\frac{1}{s}\nabla \cdot [k_g\|\nabla\bar{y}]$
$b(y,\theta)$	$\begin{cases} y - y_b & \mathbf{r} \in \partial D_1 \\ \nabla y \cdot n & \mathbf{r} \in \partial D_2 \end{cases}$

Where $k_g = e^{\theta}$.

TABLE 2. Discretized Model Operators for the Groundwater Flow Example

Operator	Definition
$[F(Y, \Theta)]_i$	$[C^{-1}]_{im}[A_{mn}(\Theta)Y_n + B_m]$
$[F(\bar{Y}, \bar{\Theta})]_i$	$[C^{-1}]_{im}[A_{mn}(\bar{\Theta})\bar{Y}_n + B_m]$
$[F_Y]_{ij}\delta Y_j$	$[C^{-1}]_{im}A_{mj}(\bar{\Theta})\delta Y_j$
$[F_\Theta]_{ij}\delta\Theta_j$	$[C^{-1}]_{im}\left[\frac{\partial A_{mn}}{\partial\Theta_j}(\bar{\Theta})\right]\bar{Y}_n\delta\Theta_j$
$[F_{YY}]_{ijk}\delta Y_j\delta Y_k$	0
$[F_{Y\Theta}]_{ijk}\delta Y_j\delta\Theta_k$	$[C^{-1}]_{im}\frac{\partial A_{mj}}{\partial\Theta_k}(\bar{\Theta})\delta Y_j\,\delta\Theta_k$
$[F_{\Theta\Theta}]_{ijk}\delta\Theta_j\delta\Theta_k$	$[C^{-1}]_{im}\left[\frac{\partial^2 A_{mn}}{\partial\Theta_j\partial\Theta_k}(\bar{\Theta})\right]\bar{Y}_n\delta\Theta_j\,\delta\Theta_k$

Summation over repeated indices is implied (from 1 to M).

where

$$k_g = e^{\bar{\theta}} \qquad \sigma_\theta{}^2 = P_{\theta\theta}(\mathbf{r}, \mathbf{r}) \tag{8e}$$

The mean head equation given here has the same general form as the deterministic flow equation, with $\bar{y}$ substituted for y, except for the presence of the second-order term. This term is obtained from the expectation of $f_{y\theta}\delta y\delta\theta$ (defined in Table 1) by introducing a second location coordinate $\mathbf{r}'$ [see *McLaughlin and Wood*, this issue, Appendix A]. The perturbation $\delta\theta$ can then be brought inside the ∇ operator as follows:

$$\overline{\delta\theta(\mathbf{r})\nabla\delta y(\mathbf{r}, t)} = \{\nabla[\overline{\delta y(\mathbf{r}, t)\delta\theta(\mathbf{r}')}]\}_{\mathbf{r}'=\mathbf{r}} = [\nabla P_{y\theta}(\mathbf{r}, \mathbf{r}', t)]_{\mathbf{r}'=\mathbf{r}}$$

The argument $\mathbf{r}'$ appearing in (8a) is set equal to $\mathbf{r}$ after the gradient of $P_{y\theta}$ is taken but before the divergence operator is applied.

Equations for the reference covariances may be obtained by substituting the operator definitions from Table 1 into the appropriate components of (17) and (18) of *McLaughlin and Wood* [this issue]:

$$\frac{s}{k_g}\frac{\partial P_{yy}}{\partial t} \simeq \nabla^2 P_{yy} + \nabla \cdot [P_{\theta y}\nabla\bar{y}] + \nabla'^2 P_{yy} + \nabla' \cdot [P_{y\theta}\nabla'\bar{y}'] \tag{9a}$$

$$\mathbf{r}, \mathbf{r}' \in D$$

$$P_{yy} = 0 \qquad \mathbf{r} \text{ or } \mathbf{r}' \in \partial D_1 \qquad \mathbf{r}' \text{ or } \mathbf{r} \in D \tag{9b}$$

$$\nabla P_{yy} \cdot \mathbf{n} = 0 \qquad \mathbf{r} \in \partial D_2 \qquad \mathbf{r}' \in D \tag{9c}$$

$$\nabla' P_{yy} \cdot \mathbf{n}' = 0 \qquad \mathbf{r}' \in \partial D_2 \qquad \mathbf{r} \in D \tag{9d}$$

$$P_{yy} = 0 \qquad \mathbf{r}, \mathbf{r}' \in D \qquad t = t_0 \tag{9e}$$

$$\frac{s}{k_g}\frac{\partial P_{y\theta}}{\partial t} \simeq \nabla^2 P_{y\theta} + \nabla \cdot [P_{\theta\theta}\nabla\bar{y}] \qquad \mathbf{r}, \mathbf{r}' \in D \tag{10a}$$

$$P_{y\theta} = 0 \qquad \mathbf{r} \in \partial D_1 \qquad \mathbf{r}' \in D \tag{10b}$$

$$\nabla P_{y\theta} \cdot \mathbf{n} = 0 \qquad \mathbf{r} \in \partial D_2 \qquad \mathbf{r}' \in D \tag{10c}$$

$$P_{y\theta} = 0 \qquad \mathbf{r}, \mathbf{r}' \in D \qquad t = t_0 \tag{10d}$$

Here primed variables such as $\mathbf{n}'$ or $\bar{y}'$ are understood to be evaluated at $\mathbf{r}'$, while unprimed variables are evaluated at $\mathbf{r}$. Similarly, primed operators are understood to act on $\mathbf{r}'$ and are evaluated at the mean values $\bar{\theta}'$ and $\bar{y}'$, while unprimed operators act on $\mathbf{r}$ and are evaluated at the mean values $\bar{\theta}$ and $\bar{y}$. The first subscript of each covariance function is associated

with $\mathbf{r}$, while the second subscript is associated with $\mathbf{r}'$. Note that the auxiliary conditions for the covariances are homogeneous because the initial and boundary heads are assumed to be known perfectly. Uncertainty enters solely through the forcing term $P_{\theta\theta}$, which accounts for the spatial heterogeneity of the log hydraulic conductivity.

The reference moment expressions of (8), (9), and (10) form a closed set of scalar partial differential equations which may be solved with techniques similar to those commonly used to solve the original groundwater flow equation. The solution process is complicated somewhat by the presence of forcing terms which depend on the covariances $P_{y\theta}$ and $P_{\theta\theta}$ and by the need to integrate (10) with respect to two spatial variables ($\mathbf{r}$ and $\mathbf{r}'$). Specific solution alternatives are discussed in more detail in the next section.

The moments of the model state are derived in the same way as those of the reference state. If the operator definitions of Table 2 are substituted into appropriate components of (19) of *McLaughlin and Wood* [this issue] the following set of coupled ordinary differential equations is obtained for the elements of the mean head vector $\bar{Y}(t)$:

$$C_{mi}\frac{d\bar{Y}_i}{dt} \simeq \left\{A_{mi} + \frac{1}{2}\left[\frac{\partial^2 A_{mi}}{\partial\Theta_k\partial\Theta_l}\right][P_{\Theta\Theta}]_{kk}\delta_{kl}\right\}\bar{Y}_i + B_m + \frac{\partial A_{mi}}{\partial\Theta_n}[P_{Y\Theta}]_{in} \qquad m = 1, \cdots, M \tag{11a}$$

$$\bar{Y}_m = [Y_0]_m \qquad t = t_0 \qquad m = 1 \cdots M \tag{11b}$$

where

$$\bar{\Theta}_m = \bar{\theta} \tag{11c}$$

Repeated indices are understood to be summed over the range from 1 to M, and all partial derivatives are evaluated at the mean values $\bar{Y}$ and $\bar{\Theta}$. Equation (11*c*) follows from the unbiasedness condition imposed on the kriging equations, as expressed in (6*b*).

Equations for the model covariances may be obtained from Table 2 and (21) and (22) of *McLaughlin and Wood* [this issue]:

$$\frac{d[P_{YY}]_{mn}}{dt} \simeq [C^{-1}]_{mk}A_{ki}[P_{YY}]_{in} + [C^{-1}]_{mk}\frac{\partial A_{ki}}{\partial\Theta_l}\bar{Y}_i[P_{\Theta Y}]_{ln} + [C^{-1}]_{nk}A_{ki}[P_{YY}]_{mi} + [C^{-1}]_{nk}\frac{\partial A_{ki}}{\partial\Theta_l}\bar{Y}_i[P_{Y\Theta}]_{ml} \qquad m, n = 1, \cdots, M \tag{12a}$$

$$[P_{YY}]_{mn} = 0 \qquad t = t_0 \qquad m, n = 1, \cdots, M \tag{12b}$$

$$C_{mi}\frac{d[P_{Y\Theta}]_{in}}{dt} \simeq A_{mi}[P_{Y\Theta}]_{in} + \frac{\partial A_{mi}}{\partial\Theta_l}\bar{Y}_i[P_{\Theta\Theta}]_{ln} \qquad m, n = 1, \cdots, M \tag{13a}$$

$$[P_{Y\Theta}]_{mn} = 0 \qquad t = t_0 \qquad m, n = 1, \cdots, M \tag{13b}$$

where

$$P_{\Theta\Theta} = \Lambda P_{ZZ}\Lambda^T \tag{13c}$$

$$[P_{ZZ}]_{nm} = P_{\theta\theta}(\mathbf{r}_n, \mathbf{r}_m) + R_{nm} \qquad n, m = 1 \cdots N \tag{13d}$$

Here again, the auxiliary conditions are homogeneous because the initial and boundary heads are assumed to be known perfectly. Uncertainty enters the model equations solely through the forcing term $P_{\Theta\Theta}$, which is influenced both by the heterogeneity of the reference system and by the sampling and estimation process.

Taken together, the model moment expressions of (11), (12), and (13) form a closed set of ordinary differential equations which can be solved with conventional techniques [*Sagar*, 1978; *Dettinger and Wilson*, 1981; *Townley*, 1983; *Hoeksema and Kitanidis*, 1984]. For the special case considered here (no structural errors) these equations are the discrete analogs of the distributed reference equations and can be solved with the same numerical algorithm. The primary difference between the reference and model equations lies in the way uncertainty is introduced. The model forcing term depends on sampling and estimation factors which have no effect on the comparable reference forcing term. Generally speaking, the estimation process causes the model's head predictions to be smoother than the reference heads (see example 2 below). This is reflected in differences between the correlation scales obtained from the model and reference covariance functions.

The reference and model moment equations provide the information needed to derive the mean prediction error (or prediction bias), which is given by

$$E[\tilde{y}(\mathbf{r}, t)] = \bar{y}(\mathbf{r}, t) - \phi(\mathbf{r})^T\bar{Y}(t) \tag{14}$$

The prediction error covariance is obtained, for the special case of no structural or discretization errors, by applying (35) and (36) of *McLaughlin and Wood* [this issue]:

$$\frac{s}{k_g}\frac{\partial P_{\tilde{y}\tilde{y}}}{\partial t} \simeq \nabla^2 P_{\tilde{y}\tilde{y}} + \nabla\cdot[P_{\partial\tilde{y}}\nabla\bar{y}] + \nabla'^2 P_{\tilde{y}\tilde{y}} + \nabla'\cdot[P_{\tilde{y}\partial}\nabla'\bar{y}'] \qquad \mathbf{r}, \mathbf{r}' \in D \tag{15a}$$

$$P_{\tilde{y}\tilde{y}} = 0 \qquad \mathbf{r} \text{ or } \mathbf{r}' \in \partial D_1 \qquad \mathbf{r}' \text{ or } \mathbf{r} \in D \tag{15b}$$

$$\nabla P_{\tilde{y}\tilde{y}}\cdot\mathbf{n} = 0 \qquad \mathbf{r}\in\partial D_2 \qquad \mathbf{r}' \in D \tag{15c}$$

$$\nabla' P_{\tilde{y}\tilde{y}}\cdot\mathbf{n}' = 0 \qquad \mathbf{r}' \in \partial D_2 \qquad \mathbf{r}\in D \tag{15d}$$

$$P_{\tilde{y}\tilde{y}} = 0 \qquad \mathbf{r}, \mathbf{r}' \in D \qquad t = t_0 \tag{15e}$$

$$\frac{s}{k_g}\frac{\partial P_{\tilde{y}\partial}}{\partial t} \simeq \nabla^2 P_{\tilde{y}\partial} + \nabla\cdot[P_{\partial\partial}\nabla\bar{y}] \qquad \mathbf{r}, \mathbf{r}' \in D \tag{16a}$$

$$P_{\tilde{y}\partial} = 0 \qquad \mathbf{r}\in\partial D_1 \qquad \mathbf{r}' \in D \tag{16b}$$

$$\nabla P_{\tilde{y}\partial}\cdot\mathbf{n} = 0 \qquad \mathbf{r}\in\partial D_2 \qquad \mathbf{r}' \in D \tag{16c}$$

$$P_{\tilde{y}\partial} = 0 \qquad \mathbf{r}, \mathbf{r}' \in D \qquad t = t_0 \tag{16d}$$

where

$$P_{\partial\partial}(\mathbf{r}, \mathbf{r}') = P_{\theta\theta}(\mathbf{r}, \mathbf{r}') - \phi_m(\mathbf{r})\Lambda_{mn}P_{\theta\theta}(\mathbf{r}_n, \mathbf{r}') - P_{\theta\theta}(\mathbf{r}, \mathbf{r}_m)\Lambda_{mn}\phi(\mathbf{r}') + \phi_m(\mathbf{r})\Lambda_{mn}P_{\theta\theta}(\mathbf{r}_n, \mathbf{r}_p)\Lambda_{pq}\phi_q(\mathbf{r}') \tag{16e}$$

All repeated subscripts in (16*e*) are summed from 1 to N. The head prediction error variance at any location $\mathbf{r}$ and time t is given by

$$\sigma_{\tilde{y}}^2(\mathbf{r}, t) = P_{\tilde{y}\tilde{y}}(\mathbf{r}, \mathbf{r}, t) \tag{17}$$

Equations (15) and (16) have the same structure as (9) and (10) and may be solved in the same way. The reference moment equations must be solved to give the mean head $\bar{y}$, which is treated as a known quantity in (15) and (16).

Solution of the Moment Equations

The reference and error moment equations developed above are linear partial differential equations which may have spatially variable coefficients. These equations can be solved in a number of ways, some more general than others. For present

purposes, we consider three particular solution approaches: Fourier transform methods, Green's function techniques, and numerical methods [*Courant and Hilbert*, 1953; *Hildebrand*, 1976; *Greenberg*, 1978]. Our emphasis here is on the relative merits of each approach for groundwater accuracy evaluation purposes. Methodological details are discussed in the cited references.

If the reference and error moment equations are defined over a domain D which is sufficiently large compared to the head correlation scale, it is convenient to assume that this domain is infinite. The moment equations can then, in certain cases, be solved with transform techniques. To illustrate the approach, we consider the reference equations for the time-invariant stationary case. These can be inferred from (8), (9), and (10):

$$\left[1 + \frac{\sigma_\theta^2}{2}\right]\nabla^2 \bar{y}(\mathbf{r}) \simeq -\frac{1}{k_g} q(\mathbf{r}) - \nabla \cdot [\nabla P_{y\theta}(\mathbf{r}, \mathbf{r}')]_{\mathbf{r}'=\mathbf{r}} \qquad (18)$$

$$\mathbf{r} \in D$$

$$\nabla^2 P_{yy}(\mathbf{r}, \mathbf{r}') \simeq -\nabla P_{y\theta}(\mathbf{r}', \mathbf{r}) \cdot \nabla \bar{y}(\mathbf{r}) \qquad (19)$$

$$\nabla^2 P_{y\theta}(\mathbf{r}, \mathbf{r}') \simeq -\nabla P_{\theta\theta}(\mathbf{r}, \mathbf{r}') \cdot \nabla \bar{y}(\mathbf{r}) \qquad (20)$$

The boundary conditions remain unchanged. If the log conductivity is stationary, the mean gradient is approximately constant, and the infinite domain assumption is introduced, the steady state equations may be written exclusively in terms of the spatial increment $\boldsymbol{\zeta} = \mathbf{r} - \mathbf{r}'$:

$$\nabla \bar{y}(\mathbf{r}) \simeq -\mathbf{J} = \text{const} \qquad (21)$$

$$\nabla_\zeta^2 P_{yy}(\boldsymbol{\zeta}) \simeq -\nabla_\zeta P_{y\theta}(\boldsymbol{\zeta}) \cdot \mathbf{J} \qquad (22)$$

$$\nabla_\zeta^2 P_{y\theta}(\boldsymbol{\zeta}) \simeq \nabla_\zeta P_{\theta\theta}(\boldsymbol{\zeta}) \cdot \mathbf{J} \qquad (23)$$

The covariance functions P_{yy}, $P_{y\theta}$, and $P_{\theta\theta}$ are defined as before with all occurrences of $\mathbf{r} - \mathbf{r}'$ replaced by $\boldsymbol{\zeta}$. The ζ subscript on the ∇ operator indicates differentiation with respect to the vector $\boldsymbol{\zeta}$. Note that the minus sign in the right-hand side of (22) is a result of the reversed order of the $\mathbf{r}$ and $\mathbf{r}'$ coordinates in the function $P_{y\theta}(\mathbf{r}', \mathbf{r})$ appearing in (19).

Equations (22) and (23) may be Fourier transformed with respect to the spatial variable $\boldsymbol{\zeta}$ to give a set of algebraic equations for the spectral densities S_{yy} and $S_{y\theta}$, which are the Fourier transforms of P_{yy} and $P_{y\theta}$, respectively [*Greenberg*, 1978; *Lumley and Panofsky*, 1964]. These transformed equations can be readily solved to give the following relationship between the head and log conductivity spectra:

$$S_{yy}(\mathbf{k}) \simeq \frac{iS_{y\theta}(\mathbf{k})[\mathbf{k} \cdot \mathbf{J}]}{\mathbf{k} \cdot \mathbf{k}} = \frac{S_{\theta\theta}(\mathbf{k})[\mathbf{k} \cdot \mathbf{J}][\mathbf{k} \cdot \mathbf{J}]}{(\mathbf{k} \cdot \mathbf{k})^2} \qquad (24)$$

where $\mathbf{k}$ is a three-dimensional wave number vector and i is the imaginary constant $(-1)^{1/2}$. Equation (24) is the expression obtained by *Bakr et al.* [1978] using a related approach based on a Fourier-Stieltjes solution of the original stochastic partial differential equation. In either case, the stationary head covariance function can be obtained by inverse Fourier transforming the spectral density [*Lumley and Panofsky*, 1964]. In one and two dimensions, restrictions must be imposed on the form of the log hydraulic conductivity covariance in order to insure that this covariance is bounded [*Bakr et al.*, 1978]. It should be noted that the transform approach can be extended to deal with transient problems if the spectra are allowed to depend on time. In this case, the governing spectral equations are ordinary differential equations with specified initial conditions [*Greenberg*, 1978].

Transform methods are convenient for solving the reference covariance equations, but they cannot be readily applied to the prediction error problem. This is because the conditioning effect of log conductivity measurements makes the error covariance function nonstationary, even when the reference covariance is stationary. Although nonstationarity can be accommodated by using spectral densities which depend on two independent wave number variables [*Newland*, 1984], this complication makes the spectral equations much more difficult to solve.

Green's function theory provides an alternative solution method which may be used to obtain either reference or error moments. The basic concepts may again be illustrated with the steady state reference equations. If, for simplicity, we neglect the second-order terms in (18) the mean head solution may be written [*Greenberg*, 1978]

$$\bar{y}(\mathbf{r}) \simeq \int_{\partial D_1} y_b(\boldsymbol{\rho}) \nabla G(\mathbf{r}; \boldsymbol{\rho}) \cdot \mathbf{n}(\boldsymbol{\rho})\, d\boldsymbol{\rho} - \frac{1}{k_g} \int_D G(\mathbf{r}; \boldsymbol{\rho}) q(\boldsymbol{\rho})\, d\boldsymbol{\rho} \qquad (25)$$

Here the scalar G is the Green's function (or impulse response) obtained by solving the deterministic version of (18) (with $\sigma_\theta^2 = P_{y\theta} = 0$) when the forcing function $q(\mathbf{r})/k_g$ is a Dirac delta function at location $\boldsymbol{\rho}$. The first term in (25) accounts for boundary conditions, while the second term accounts for the effect of the interior forcing function. Note that the boundary term implicitly incorporates the no-flux condition imposed on ∂D_2.

The Green's function technique is particularly attractive for the time-invariant case when all the reference and error moment equations have the basic same structure. The reference covariances may, for example, be obtained by applying the technique to (19) and (20):

$$P_{y\theta}(\mathbf{r}, \mathbf{r}') \simeq \int_D G(\mathbf{r}; \boldsymbol{\rho})[\nabla_\rho P_{\theta\theta}(\boldsymbol{\rho}, \mathbf{r}')] \cdot [\nabla_\rho \bar{y}(\boldsymbol{\rho})]\, d\boldsymbol{\rho} \qquad (26)$$

$$P_{yy}(\mathbf{r}, \mathbf{r}') \simeq \int_D G(\mathbf{r}; \boldsymbol{\rho})[\nabla_\rho P_{y\theta}(\mathbf{r}', \boldsymbol{\rho})] \cdot [\nabla_\rho \bar{y}(\boldsymbol{\rho})]\, d\boldsymbol{\rho} \qquad (27)$$

The ρ subscript on the ∇_ρ operator indicates differentiation with respect to the spatial integration variable $\boldsymbol{\rho}$. Note that the spatial variable $\mathbf{r}'$ appears as a source term argument in both (26) and (27). The Green's function does not depend on $\mathbf{r}'$. A general expression for the variance of the reference head may be obtained by substituting (26) into (27) and setting $\mathbf{r}' = \mathbf{r}$. If the mean head gradient is approximately constant this general expression may be approximated by

$$\sigma_y^2(\mathbf{r}) \simeq \int_D \int_D G(\mathbf{r}; \boldsymbol{\rho}) G(\mathbf{r}; \boldsymbol{\rho}')[\nabla \cdot \nabla' P_{\theta\theta}(\boldsymbol{\rho}, \boldsymbol{\rho}')] \cdot [\nabla \bar{y}(\boldsymbol{\rho}) \cdot \nabla' \bar{y}(\boldsymbol{\rho}')]\, d\boldsymbol{\rho}\, d\boldsymbol{\rho}' \qquad (28)$$

The above equations provide convenient expressions for the desired moments of y if the Green's function can be found. This can be a difficult task, particularly for general problems with irregular boundaries. In some cases, simplifications can be introduced which will yield specialized problems with known Green's functions. If, for example, the domain D is large enough to be considered infinite the three-dimensional Green's function for the problem formulated here is [*Hildebrand*, 1976]

$$G(\mathbf{r}, \boldsymbol{\rho}) = -\frac{1}{4\pi} \frac{1}{|\mathbf{r} - \boldsymbol{\rho}|} \qquad (29)$$

Explicit expressions for the reference mean and variance may be obtained by substituting this Green's function into (25) and (28). Since the Green's function method can handle nonstationary source terms, it may be applied in exactly the same way to the error moment equations.

Dagan [1982*a*] presents a Green's function analysis which produces mean and variance expressions equivalent to those given in (25) and (28). His approach is based on a Neuman series expansion of a closed-form solution to the original stochastic partial differential equation. It should be noted that Green's function methods can be extended to transient problems, although the time-dependent Green's functions which are required in this case are generally difficult to derive without resorting to numerical techniques [*Dagan*, 1982*b*].

The transform and Green's function approaches are both attractive solution alternatives for certain specialized problems. More general problems must be solved with numerical methods which are not forced to make restrictive assumptions for the sake of analytical convenience. The moments presented in the examples discussed later in this paper were, for example, obtained by using a Galerkin finite element technique to solve both the reference and error moment equations [*McLaughlin*, 1985; *Pinder and Gray*, 1977].

If a Galerkin procedure is adopted, the distributed mean equation is solved in the same way as the deterministic model equation, yielding a discrete set of ordinary differential equations similar in form to (11). The distributed covariance equations must be treated somewhat differently, since the covariance functions depend on the two independent spatial arguments $\mathbf{r}$ and $\mathbf{r}'$. These functions are approximated by expressions containing two interpolation functions, one for each argument [*Courant and Hilbert*, 1953]. An example is the approximation for P_{yy}:

$$P_{yy}(\mathbf{r}, \mathbf{r}', t) \simeq [\hat{P}_{yy}]_{ij}\psi_i(\mathbf{r})\psi_j(\mathbf{r}') \tag{30}$$

where ψ_i is the interpolation function associated with node i of the computational grid and $[\hat{P}_{yy}]_{ij}$ is the discrete covariance between nodes i and j. The ψ interpolation functions need not be the same as the ϕ functions used in (3). In fact, the computational grid used to solve the distributed moment equations can generally be significantly less detailed than the grid used in a deterministic model with highly variable inputs. This is because the mean and covariance functions vary relatively smoothly compared to the stochastic variables. A grid spacing of one correlation scale, which is too large for a Monte Carlo simulation [*Ababou*, 1988], is generally adequate for covariance functions which vary linearly over this scale (see *Graham and McLaughlin* [1988] for a direct comparison of Monte Carlo and moment equation discretization requirements).

The discretized covariance solutions are obtained by substituting approximations such as (30) into each of the covariance equations. If an equation only contains derivatives with respect to $\mathbf{r}$, it is integrated over $\mathbf{r}$ for each nodal value of $\mathbf{r}'$. That is, $\mathbf{r}'$ is successively set equal to the node coordinates $\mathbf{r}_1$, $\mathbf{r}_2, \cdots, \mathbf{r}_K$, where K is the number of non-Dirichlet grid nodes. This integration follows the usual weighted residuals procedure, producing K ordinary differential equations for each of the K values of $\mathbf{r}'$ [*Pinder and Gray*, 1977]. The resulting K^2 ordinary differential equations in K^2 unknowns have the same form as (13), although the coefficient values are generally different.

If a covariance equation contains derivatives with respect to both $\mathbf{r}$ and $\mathbf{r}'$, it is integrated first over $\mathbf{r}$, with $\mathbf{r}'$ carried as a parameter. Here again, a standard weighted residuals procedure is used to carry out the integration. The result is a set of K partial differential equations which contain only $\mathbf{r}'$ spatial derivatives. Each of these equations is then integrated over $\mathbf{r}'$. The resulting K^2 ordinary differential equations in K^2 unknowns have the same form as (12).

The discretized reference, moment, and error moment equations can be decomposed with the "square root" algorithm described in Appendix B of *McLaughlin and Wood* [this issue] and then solved as coupled sets of ordinary differential equations. Other methods for solving discretized moment equations are described by *Sagar* [1978], *Dettinger and Wilson* [1981], *Townley* [1983], and *Hoeksema and Kitanidis* [1984]. It should be noted that all of these methods require unusually large amounts of computer memory to store the covariance matrices which result when grid sizes exceed a few thousand (see the last section of *McLaughlin and Wood* [this issue]). This is a major limitation of the numerical approach which needs to be resolved before large-scale three-dimensional analyses can be undertaken.

The above discussion illustrates one of the conceptual advantages of the distributed parameter viewpoint. The solution techniques described by *Bakr et al.* [1978], *Dagan* [1982*a*, *b*], and *Sagar* [1978] can all be viewed as different ways to solve the same set of distributed parameter moment equations. The distributed approach provides a general theory which encompasses all of these techniques and is, moreover, not forced to rely on any approximations other than the important small perturbation assumption. Additional assumptions imposed to achieve solutions are not inherent to the method and can be tailored to fit the unique characteristics of each application. This provides considerable flexibility which permits the investigator to mix different techniques to achieve the most efficient solution to any given problem.

EXAMPLES

The numerical examples described in this section are intended to illustrate how the distributed parameter approach to accuracy evaluation can be applied. The first example considers reference moments in a three-dimensional region subject to boundary conditions which create a nearly uniform mean head gradient. The results for this problem are compared to the predictions of the infinite domain stationary theory described by *Bakr et al.* [1978]. The second example considers prediction error moments for a simplified two-dimensional aquifer development problem. This problem focuses on sampling design and estimation issues. It is similar, in some respects, to the two-dimensional well pumping problem examined by *Dagan* [1982*a*, pp. 827–829]. Both examples rely on the state and moment equations developed in the first part of this paper. All moment equations are solved with a modified version of the finite element algorithm described by *Babu et al.* [1982].

Reference Moments for a Quasi-Stationary Three-Dimensional Problem

This example investigates the reference moments for a steady state problem which approximates stationary conditions near the center of a three-dimensional region. The reference system is described by (1), where y is the hydraulic head, θ is the log hydraulic conductivity, and dy/dt and q are both zero. The solution region is a cube with constant, perfectly known head boundary conditions on sides A and A′ and zero normal flux boundary conditions on the remaining sides (see Figure 1*a*). Since we are concerned with steady state re-

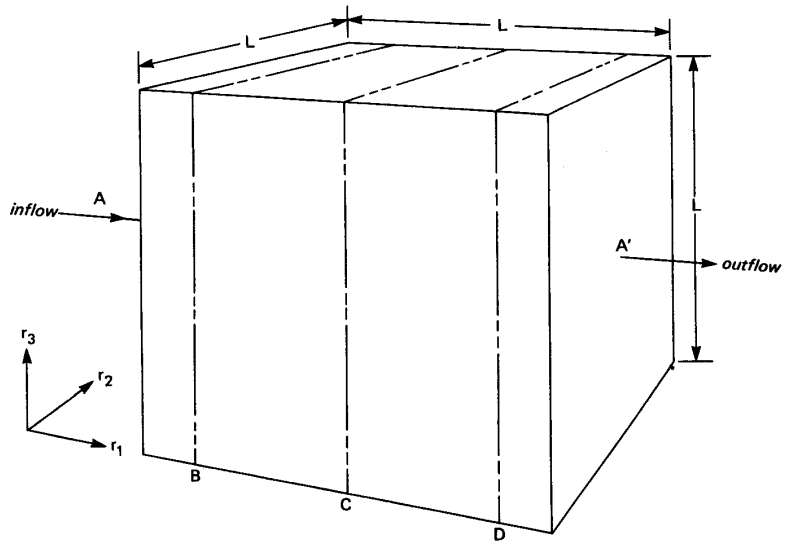

a) Flow region

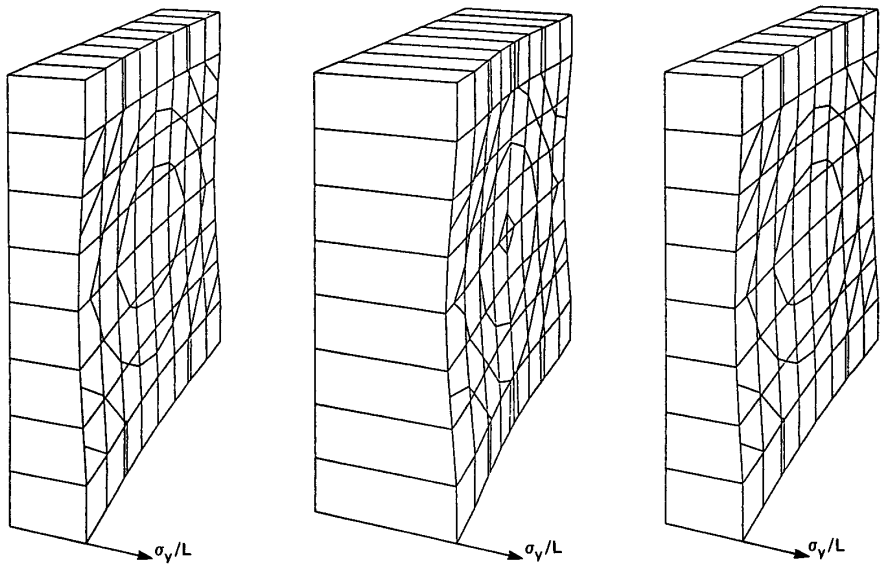

b) Section B c) Section C d) Section D

Fig. 1. Steady state reference head standard deviation surfaces for selected sections of the example 1 flow region (standard deviation scales exaggerated 5 ×).

sults, the only uncertain input is the log hydraulic conductivity, which is assumed to have a constant mean and variance with the following stationary isotropic exponential covariance function:

$$P_{\theta\theta}(\mathbf{r} - \mathbf{r}') = \sigma_\theta^2 \exp(-|\mathbf{r} - \mathbf{r}'|/\lambda) \quad (31)$$

It is convenient to normalize the variables in the governing equation so that all inputs and results are unitless. Table 3 lists the nominal set of normalized inputs used to compute the reference moments for this example. Note that all length units are divided by L, the length of the solution region, and all time units are divided by the ratio L/k_g, where k_g is defined as in (8*e*).

The boundary conditions for this example are designed to give a nearly uniform head gradient along the r_1 axis extending from side A to side A′ in Figure 1. In this case, the conditions needed to apply (21)–(23) hold sufficiently far from the boundaries, and we would expect to obtain reference head variances at the center of the cube which approximate the infinite domain results derived by *Bakr et al.* [1978]. Figures 1 and 2 present the results of our finite domain computations for the nominal case. These are based on a finite element solution of (10)–(12), discretized over a regular 9 by 9 by 9 grid. Figures 1*b*–1*d* show the normalized head standard deviations computed at the three vertical sections labeled B, C, and D in Figure 1*a*. The standard deviation axis is magnified

TABLE 3. Nominal Inputs for Examples 1 and 2

Normalized Variable	Example 1	Example 2
Storage coefficient	···	0.01
Pumpage	···	$q\varepsilon/k_g = 0.006$
θ definition	$\log_e$ conductivity	$\log_e$ transmissivity
θ correlation scale	$\lambda_\theta/L = 0.1$	$\lambda_\theta/\varepsilon = 10.0$
θ standard deviation	$\sigma_\theta = 1.0$	$\sigma_\theta = 1.0$
θ measurement error standard deviation	···	$\sigma_\omega = 0.1$
Regional head gradient	$(h_A - h_{A'})/L = 1.0$	···

The mean of θ is assumed to be spatially invariant. Measurement errors are independent and zero mean with equal standard deviations (σ_ω). The nominal sampling configuration for example 2 is strategy D. The nominal kriging weights for example 2 are derived from the correct reference log transmissivity covariance function.

by a factor of 5.0 to better illustrate variability over the vertical plane. It is apparent that the head standard deviation is nearly uniform in any given plane, with a slight dip near the center.

Figure 2 shows the head mean and standard deviation profiles along the AA′ axis. As expected, the mean head gradient is nearly uniform, and the standard deviation approaches a constant value near the center of the cube. The center head standard deviations obtained for various values of σ_θ, λ_θ, and J are compared with the infinite domain *Bakr et al.* [1978] results in Figure 3. The match is quite close when the correlation scale is 0.1 or less, suggesting that the infinite domain approximation is reasonable, for this example, at distances greater than five correlation scales from a specified head boundary. This is consistent with stochastic simulation results reported by *Ababou* [1988]. The head standard deviation decrease is smaller than the infinite domain value when the correlation scale increases, reflecting the increased effect of the known (zero variance) boundary conditions. The linear dependence on the ratio $\sigma_\theta\lambda_\theta J/L$ which is observed in both the finite and infinite domain cases is a result of the small perturbation approximation which is common to both methods. Note that the grid spacing required in this problem is determined by the variability of the log conductivity and head covariance functions rather than by the variability in the stochastic variables (see the comment on grid resolution in the preceding section).

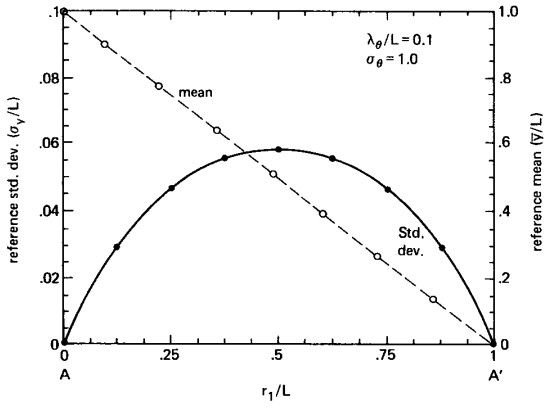

Fig. 2. Profiles of steady state reference head mean and standard deviation along section AA′ of the example 1 flow region.

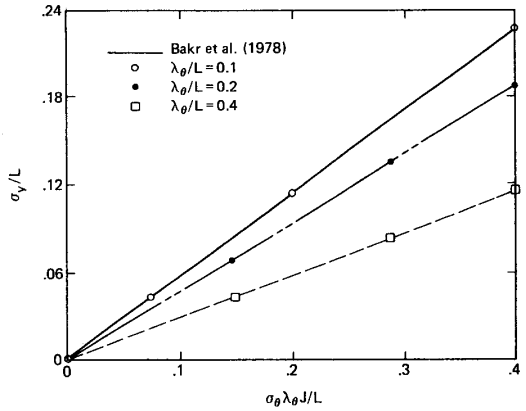

Fig. 3. Steady state reference head standard deviation at the center of the example 1 flow region.

Sensitivity tests confirmed that a grid spacing of about one correlation scale is satisfactory for this problem.

Numerical experiments similar to the one outlined above could be used to test the applicability of infinite domain, constant gradient approximations in other more complex situations. Comparisons for anisotropic log conductivity covariances such as those considered by *Gelhar and Axness* [1983] and for two-dimensional problems such as those considered by *Mizell et al.* [1982] would be particularly informative. The numerical grid for the anisotropic case would, however, have to be significantly larger than the 729 node network used here to provide adequate comparisons for anisotropy ratios larger than about 2 to 1. Since our present interest is primarily in sampling and estimation issues, we turn, instead, to our second example.

Prediction Error Moments for an Aquifer Development Problem

This example is concerned with the accuracy of vertically averaged drawdown predictions obtained from a two-dimensional groundwater flow model [*Babu et al.*, 1982]. The model's predictions are intended to provide an indication of the impact of increased pumpage from a confined aquifer used for domestic and agricultural water supply. In such situations, pumpage is often distributed over a significant fraction of the aquifer depth, and management interest is usually focused on vertically averaged quantities. If we assume that vertical variability is sufficiently small for the two-dimensional approximation to be justified, it is reasonable to evaluate model accuracy relative to a two-dimensional reference system. This allows us to neglect structural errors and to base the accuracy analysis on the simplified moment equations discussed in the previous sections of this paper. In applications where vertical variability is important it may be necessary to adopt a fully three-dimensional reference system description. Although the hypothetical example outlined below is highly simplified, it addresses many of the accuracy issues raised in more complex real-world applications [*McLaughlin and Johnson*, 1987]. These include important questions regarding the effect of spatial variability on prediction accuracy and the relative benefit of alternative sampling and estimation strategies.

The aquifer to be modeled is a square region of uniform thickness ε and length 100ε. The model flow equation is dis-

Sampling strategy	no. of wells	well locations
A	1	●
B	3	A + ▽
C	5	B + ○
D	9	C + □
E	13	D + △
F	17	E + X

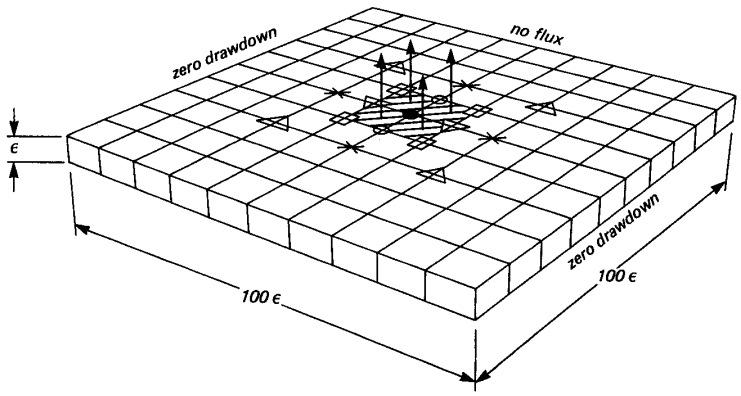

Fig. 4. Aquifer, grid, and sampling geometry for example 2.

cretized over the regular 11 by 11 node grid illustrated in Figure 4. The dependent variable of interest is the drawdown, defined as the difference between the hydraulic head at time t_0 (prior to the increase in pumpage) and the hydraulic head at some subsequent time $t > t_0$. Zero drawdown conditions apply on the boundaries parallel to the r_1 axis, while zero normal flux conditions apply on the boundaries parallel to the r_2 axis. The additional pumpage to be investigated is assumed to be distributed uniformly over a 20ε by 20ε well field located in the center of the region.

Since the initial drawdown is zero by construction, the only uncertain reference input is the log transmissivity, which is assumed to have a constant mean and variance with a stationary isotropic exponential covariance function similar to (31) but with $\mathbf{r}$ and $\mathbf{r}'$ defined over a two-dimensional region. The nodal log transmissivity values required by the model are estimated with a kriging algorithm, using noisy measurements collected at sampling points clustered near the central well field. Figure 4 defines six different sampling configurations which include from 1 to 17 log transmissivity measurement locations. Sampling strategy D is defined, for sensitivity analysis purposes, to be the nominal. The log transmissivity measurements may be noisy, and the weights used in the kriging algorithm may be suboptimal due to errors in specifying the log transmissivity variance or correlation scale.

As in the previous example, it is convenient to express all inputs and results in terms of nondimensional quantities. In this case, all length units are normalized by ε and all time units are normalized by ε/k_g. The complete set of nominal inputs is summarized in Table 3. The normalized log transmissivity mean is assumed to be constant, primarily for computational convenience, and the log transmissivity standard deviation is set equal to 1.0 in order to stay within the limits of the small perturbation assumption. If the actual range of log transmissivities were significantly larger than this, the increased variability would probably have to be handled by allowing the mean to vary over space [*McLaughlin and Wood*, this issue]. The nominal log transmissivity correlation scale of 10ε is relatively small compared to the domain size but large enough to produce significant head variability.

In this example, the primary influences on prediction accuracy are the degree of spatial variability assumed, the sampling strategy adopted, and the accuracy of assumptions made in deriving the input estimation algorithm. The results presented here illustrate the effects of each of these factors on the mean and standard deviation of the normalized prediction error. It is useful to begin by examining the aquifer's steady state behavior for a typical set of random inputs. Figure 5*a* shows a contour plot of a representative log transmissivity field having the statistical properties given in Table 3. The resulting steady state drawdown field is shown in Figure 5*c*. The log transmissivity field was generated with a turning bands algorithm similar to the one described by *Journel and Huijbreghts* [1978] and *Mantoglou* [1987], while the drawdown field was simulated with the finite element model described by *Babu et al.* [1982]. The drawdown contour plot clearly illustrates the smoothing that takes place when random transmissivity variations are attenuated by the groundwater flow equation.

Figure 5*b* shows the estimated log transmissivity field obtained by kriging noisy log transmissivity measurements sampled from the reference field of Figure 5*a*. The measurements were taken at the nominal well locations, and the kriging algorithm was derived from perfect knowledge of the reference covariance function. The steady state drawdown predictions obtained from the kriged field are plotted in Figure 5*d*. The drawdown predictions are reasonably good considering the poor description of the log transmissivity field provided by the kriged well observations. The insensitivity of these predictions to transmissivity estimation error is a natural consequence of the smoothing behavior mentioned above.

The distributed parameter moment equations provide a convenient way to quantify behavior such as that observed in Figure 5 without resorting to stochastic simulation. This is

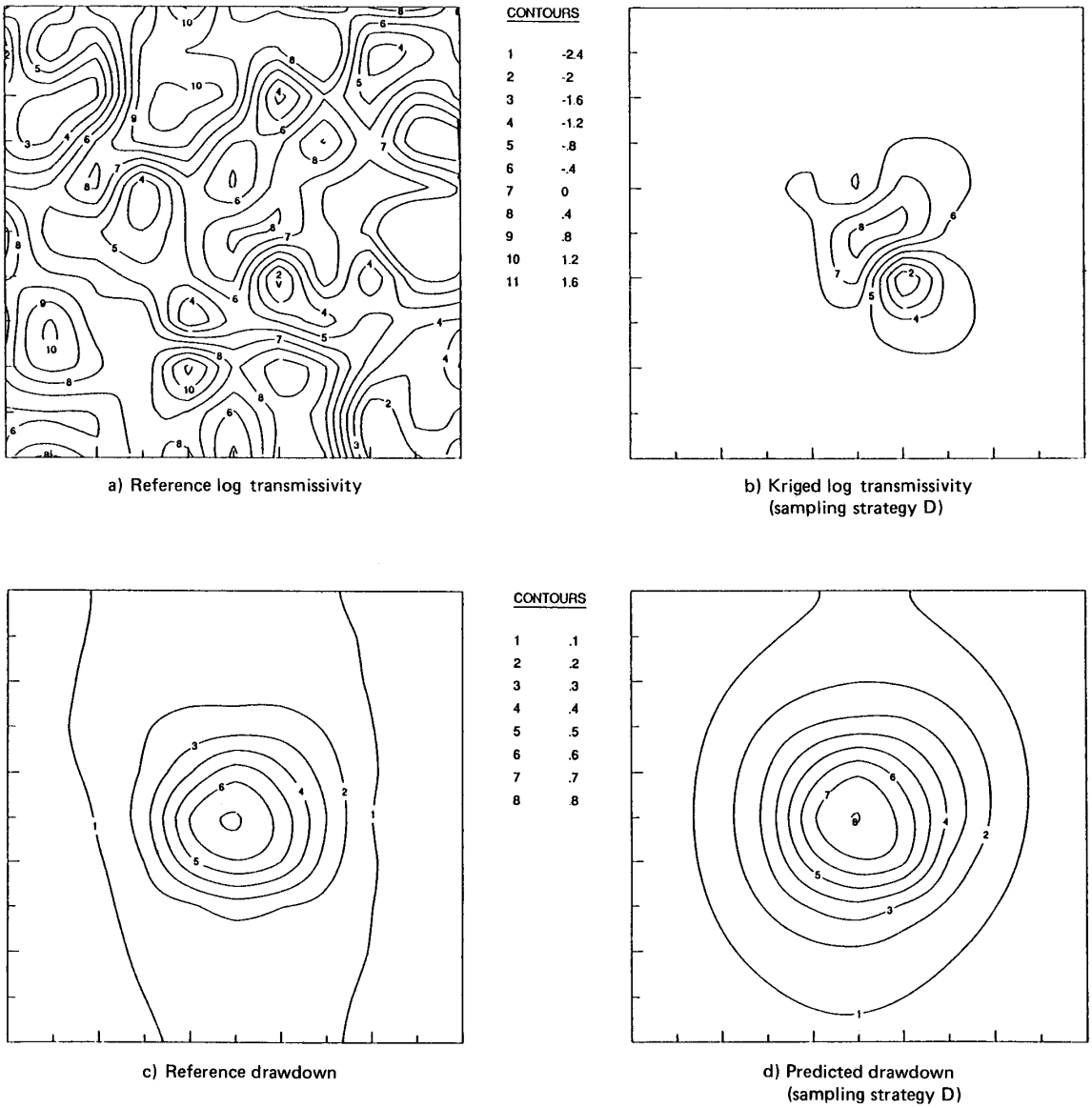

Fig. 5. Typical single replicate log transmissivity and drawdown contours for example 2.

illustrated in Figures 6 and 7, where normalized prediction error standard deviation surfaces are plotted for three different times and two different sampling strategies. These surfaces were obtained by solving the mean and covariance equations presented earlier in this paper with a finite element algorithm discretized over the 11 by 11 node grid of Figure 4. The surface plotted at the final time is essentially equivalent to the steady state result. Note that the vertical scales have been exaggerated by a factor of 10.0 to provide better definition. Although the error standard deviation surfaces have sharp peaks at the center of the well field, the distributed pumping stress gives finite mean head gradients at the center node. This is important because the linearized moment equations yield finite variances only if the mean head gradients are finite. The maximum error standard deviation obtained for nominal conditions (evaluated at the center node and the final time) is about 14% of the mean drawdown for sampling strategy D and about 7% of the mean drawdown for strategy F.

The effect of sampling strategy on prediction accuracy can be seen by comparing the error moments obtained for different sampling configurations. Figure 8 shows the decrease in the prediction error mean and standard deviation obtained under nominal conditions when the number of log transmissivity samples is increased from 1 to 17. The letter next to each plotted point refers to one of the sampling strategies defined in Figure 4. Given the placement of the sampling points associated with each strategy, the curves in Figure 8 are probably good approximation to the Pareto optimal frontiers for the two error versus sampling effort trade-offs. That is, any other strategy based on between 1 and 17 samples can be expected to lie on or above these curves. Those lying above both curves will be clearly inferior since a strategy which falls on the

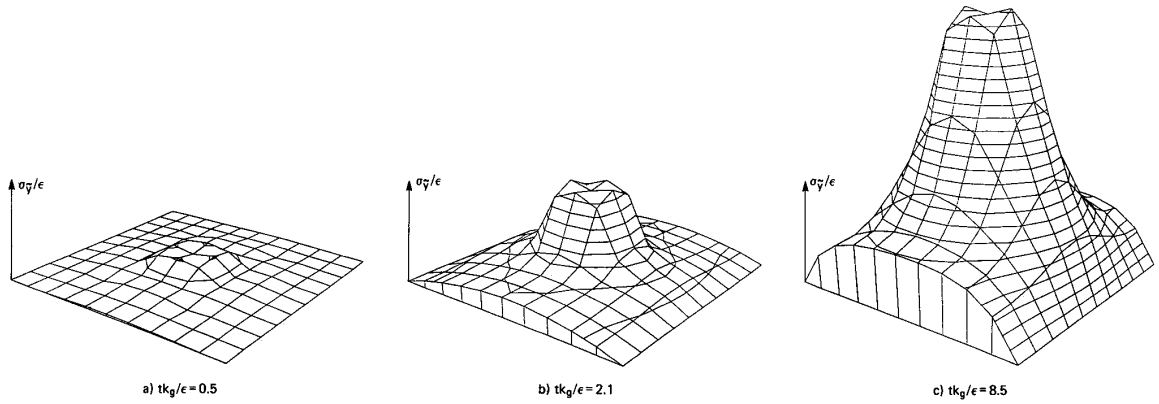

Fig. 6. Prediction error standard deviation surface for sampling strategy D of example 2 (standard deviation scales exaggerated 10 ×).

curves will give less error with no more sampling effort. Comparisons of this type can be used to decide on the size and configuration of a proposed sampling program. It is interesting to note, for example, that increased sampling effort gives relatively little improvement in the prediction error mean and gives much diminished improvement in the prediction error standard deviation for sample sizes above 10 to 15.

The effects of spatial variability on prediction accuracy are shown in Figure 9, which plots the prediction error mean and standard deviation versus the normalized log transmissivity standard deviation. Figure 9 indicates, as expected, a consistent increase in the prediction error moments as the log transmissivity standard deviation grows. The curvature observed at higher values of σ_θ is due to the effect of the second-order terms in the mean equation. Although measurement error has practically no effect on the mean error, it causes the error standard deviation curve to bend upward at low values of σ_θ.

A number of other trade-offs and sensitivities may be used to gain insight about the various factors which influence prediction accuracy. An investigation of the effect of incorrectly specified log transmissivity moments on the weights of the kriging algorithm indicated, for example, that the algorithm is very robust to such errors for the nominal sampling strategy. This is not surprising considering that the sampling points for this strategy are clustered close together in the region where estimation errors have the most impact on prediction accuracy. The importance of optimal kriging weights increases when the sampling points are farther apart and the model is forced to depend more on the kriging algorithm's interpolation procedure. Results of this type can be used to decide how to allocate limited resources to the different aspects of a modeling study. In a real application, other sources of uncertainty such as boundary condition errors would also have to be considered. Although such enhancements increase the computational effort required to obtain prediction error statistics, they fall well within the capabilities of the general theory outlined by *McLaughlin and Wood* [this issue].

Conclusions

Although the examples described above are admittedly simplified, they illustrate some of the principal advantages of a distributed approach to accuracy evaluation. This approach allows spatial variability and uncertainty to be represented in a continuous way which does not depend on a particular analytical or numerical solution scheme. The prediction error moment equations which result have a form which is very similar to the form of the original groundwater equation. The error mean and covariance obtained by solving the moment equations propagate through space and time in a predictable way, giving a quantitative measure of the evolution of uncertainty. Since the error moments depend on the sampling configuration, input estimation technique, and discretization scheme used to develop model predictions, they provide a convenient basis for comparing alternative modeling strategies. Sensitivity results such as those described in example 2 give a good feeling for the relative value of additional field measurements and improved estimation algorithms. They also indicate, in advance, whether a modeling study will be able to adequately answer the management questions which motivated it in the first place.

The theory outlined by *McLaughlin and Wood* [this issue] is sufficiently general to be applied to groundwater transport

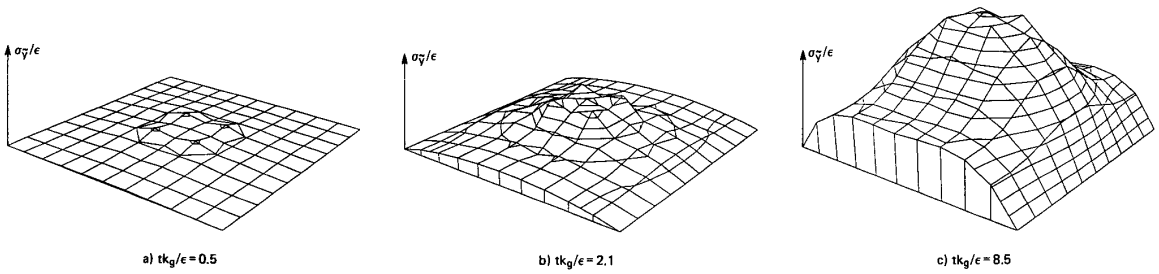

Fig. 7. Prediction error standard deviation surface for sampling strategy F of example 2 (standard deviation scales exaggerated 10 ×).

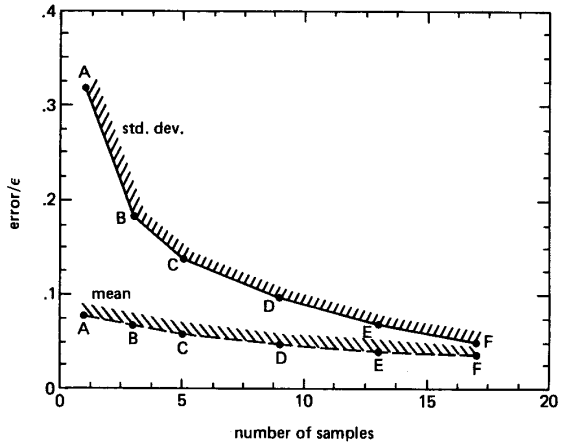

Fig. 8. Effect of sampling strategy on prediction error for example 2.

as well as saturated groundwater flow [*Graham and McLaughlin*, 1988]. The procedure for accomplishing this is similar to the one outlined earlier in this paper. Reference, model, measurement, and estimation equations need to be defined, statistical models need to be introduced for all random quantities, and differential equations for the prediction error moments need to be derived. In the case of transport the primary source of spatial variability and uncertainty is the reference groundwater velocity. If the velocity field is assumed to be at steady state, it can be treated as a time-invariant random input similar to θ. If, in addition, the velocity statistics are assumed to be stationary, they can be derived with the transform approach described by *Gelhar and Axness* [1983].

Another application which deserves mention is the generalization of the theory to provide for real-time recursive estimation of changing groundwater conditions. This problem may be posed in terms of distributed parameter Kalman filtering [*Stavroulakis*, 1983], with periodic measurements used to update estimates of conductivity, head, concentration, or other distributed state variables. Distributed parameter filters can be viewed as interpolation algorithms which rely on spatial and temporal correlations derived from the governing flow and transport equations. In this sense, distributed estimation is a natural extension of kriging, which only considers spatial correlations derived from sample statistics.

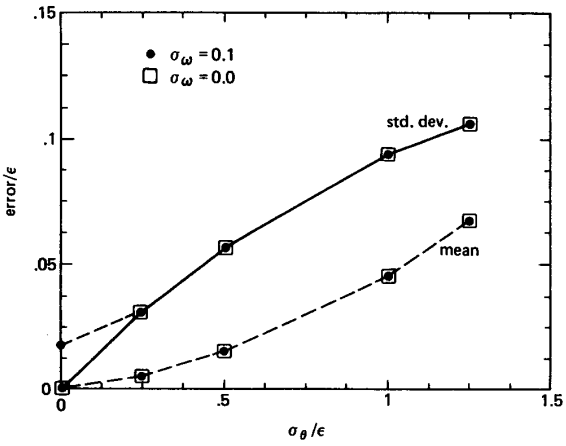

Fig. 9. Effect of log transmissivity standard deviation on prediction error for sampling strategy D of example 2.

In the end, one of the major advantages of the distributed parameter approach may be the change in viewpoint it provides. It allows us to formulate stochastic groundwater problems in much the same way as traditional groundwater problems: in terms of partial differential equations defined over distributed (nondiscretized) regions with continuously variable properties. This helps to make stochastic techniques seem a natural extension of familiar deterministic modeling, rather than a radical departure. It also focuses attention on the physical origins of variability and uncertainty. We need to understand these better before we can expect to take full advantage of the information contained in limited field observations of complex groundwater systems.

NOTATION

$A(\Theta)$, $B(Q, Y_b)$, $C(S)$ model equation coefficient matrices.
D spatial domain of interest.
∂D_1, ∂D_2 specified head and zero flux portions of the boundary of D.
$G(\mathbf{r}, \boldsymbol{\rho})$ time-invariant Green's function giving response at $\mathbf{r}$ due to an impulse at $\boldsymbol{\rho}$.
$i = (-1)^{1/2}$.
$\mathbf{J}$ hydraulic head gradient vector.
$\mathbf{k}$ Fourier wave number vector.
k_g reference hydraulic conductivity geometric mean.
K number of non-Dirichlet nodes in the computational grid used to discretize the distributed moment equations.
L domain length.
$\mathbf{n}(\mathbf{r})$ normal to ∂D_2 at $\mathbf{r}$.
M number of nodes in model computational grid, also dimensionality of Y and Θ.
N number of scalar measurements in Z.
$P_{uv}(\mathbf{r}, \mathbf{r}', t)$ cross covariance between the generic distributed variables $u(\mathbf{r}, t)$ and $v(\mathbf{r}', t)$.
$P_{UV}(t)$ cross covariance between the generic discrete variables $U(t)$ and $V(t)$.
$\hat{P}_{\Theta Z}$, $\hat{P}_{ZZ}$ estimated covariance matrices used to compute kriging weights.
$[\hat{P}_{uv}]_{ij}$ spatially discretized approximation to the distributed cross covariance P_{uv}.
$q(\mathbf{r}, t)$, $Q(t)$ reference (distributed) and model (discretized) forcing terms.
$\mathbf{r}$, $\mathbf{r}'$ spatial coordinate vectors.
R measurement error covariance matrix.
$s(\mathbf{r})$, S reference (distributed) and model (discretized) storage coefficients.
$S_{uv}(\mathbf{k})$ cross-spectral density between the generic distributed variables u and v.
t time.
t_0 initial time.
u N-dimensional vector with every element equal to 1.
$\bar{u}$, $\bar{U}$ mean of a generic variable u or U.
$y(\mathbf{r}, t)$, $Y(t)$ reference (distributed) and model (discretized) hydraulic heads.
$\tilde{y}(\mathbf{r}, t)$ model prediction error.
$y_b(\mathbf{r})$ reference head specified on ∂D_1.
$y_0(\mathbf{r})$, Y_0 reference and model initial heads.
Z vector of $\log_e$ hydraulic conductivity measurements.

δ_{ij} function equal to 1 if $i = j$ and equal to zero otherwise.
δu, δU perturbation of a generic variable about its mean $\bar{u}$ or $\bar{U}$.
ε aquifer thickness.
$\phi(\mathbf{r})$, $\psi(\mathbf{r})$ vectors of finite element interpolation (shape) functions.
Γ, Λ linear estimator weighting matrices.
λ correlation scale.
μ Lagrange multiplier used in kriging equations.
Ω measurement error vector.
$\theta(\mathbf{r}) \cdot \Theta$ reference (distributed) and model (discretized) $\log_e$ hydraulic conductivities.
σ_θ^2, $\sigma_{\tilde{y}}^2$ variances of θ and y.
∇ spatial gradient operator.

Acknowledgments. The research described in this paper was partially supported by a U.S. Geological Survey Ph.D. dissertation grant and a National Science Foundation grant (ECE-8514987), both awarded to the first author, and an Andrew W. Mellon Foundation grant ("Influence of aquifer variability on modeling groundwater contamination from hazardous waste") awarded to the second author. The authors also appreciate the helpful comments provided by Lynn Gelhar, Roger Beckie, and Rachid Ababou.

References

Ababou, R., Three-dimensional flow in random porous media, Ph.D. thesis, Mass. Inst. of Technol., Cambridge, 1988.

Babu, D. K., G. F. Pinder, and D. K. Sunada, A three-dimensional hybrid finite element-finite difference scheme for groundwater simulation, in *Proceedings of the 10th IMACS World Congress*, vol. 2, pp. 292–294, Montreal, Quebec, Canada, 1982.

Bakr, A. A., L. W. Gelhar, A. L. Gutjahr, and J. R. MacMillan, Stochastic analysis of spatial variability in subsurface flows, 1, A comparison of one- and three-dimensional flows, *Water Resour. Res.*, *14*(2), 263–271, 1978.

Carrera, J., and S. P. Neuman, Estimation of aquifer parameters under transient and steady state conditions, 1, Maximum likelihood method incorporating prior information, *Water Resour. Res.*, *22*(2), 199–210, 1986.

Chu, W.-S., E. W. Strecker, and D. P. Lettenmaier, An evaluation of data requirements for groundwater contaminant transport modeling, *Water Resour. Res.*, *23*(3), 408–424, 1987.

Clifton, P. M., and S. P. Neuman, Effects of kriging and inverse modeling on conditional simulation of the Avra Valley aquifer in southern Arizona, *Water Resour. Res.*, *18*(4), 1215–1234, 1982.

Cooley, R. L., A method of estimating parameters and assessing reliability for models of steady state groundwater flow, 1, Theory and numerical properties, *Water Resour. Res.*, *13*(2), 318–324, 1977.

Cooley, R. L., A method of estimating parameters and assessing reliability for models of steady state groundwater flow, 2, Application of statistical analysis, *Water Resour. Res.*, *15*(3), 603–617, 1979.

Courant, R., and D. Hilbert, *Methods of Mathematical Physics*, Wiley-Interscience, New York, 1953.

Dagan, G., Stochastic modeling of groundwater flow by unconditional and conditional probabilities, 1, Conditional simulation and the direct problem, *Water Resour. Res.*, *18*(4), 813–833, 1982*a*.

Dagan, G., Analysis of flow through heterogeneous random aquifers, 2, Unsteady flow in confined formations, *Water Resour. Res.*, *18*(5), 1571–1585, 1982*b*.

Dettinger, M. D., and J. L. Wilson, First-order analysis of uncertainty in numerical models of groundwater flow, 1, Mathematical development, *Water Resour. Res.*, *17*(1), 149–161, 1981.

Freeze, R. A., A stochastic-conceptual analysis of one-dimensional groundwater flow in nonuniform homogeneous media, *Water Resour. Res.*, *11*(5), 725–741, 1975.

Gelhar, L. W., Stochastic subsurface hydrology from theory to applications, *Water Resour. Res.*, *22*(9), 135S–145S, 1986.

Gelhar, L. W., and C. L. Axness, Three dimensional stochastic analysis of macrodispersion in aquifers, *Water Resour. Res.*, *19*(1), 161–180, 1983.

Graham, W., and D. McLaughlin, A comparison of numerical solution techniques for the stochastic analysis of nonstationary transient subsurface mass transport, in *Proceedings of the 7th International Conference on Computational Methods in Water Resources*, Computational Mechanics Publishers, Southampton, England, 1988.

Greenberg, M. D., *Foundations of Applied Mathematics*, Prentice-Hall, Englewood Cliffs, N. J., 1978.

Gutjahr, A., Stochastic models of subsurface flow: Log linearized Gaussian models are "exact" for covariances, *Water Resour. Res.*, *20*(12), 1909–1912, 1984.

Hildebrand, F. B., *Advanced Calculus for Applications*, Prentice-Hall, Englewood Cliffs, N. J., 1976.

Hoeksema, R. J., and P. K. Kitanidis, An application of the geostatistical approach to the inverse problem in two-dimensional groundwater modeling, *Water Resour. Res.*, *20*(7), 1003–1020, 1984.

Journel, A. G., and Ch. I. Huijbregts, *Mining Geostatistics*, Academic, San Diego, Calif., 1978.

Kitanidis, P., Parameter uncertainty in estimation of spatial functions: Bayesian analysis, *Water Resour. Res.*, *22*(4), 499–507, 1986.

Lumley, J. L., and H. A. Panofsky, *The Structure of Atmospheric Turbulence*, John Wiley, New York, 1964.

Mantoglou, A., Digital simulation of multivariate two- and three-dimensional stochastic processes with a spectral turning bands method, *Math. Geol.*, *19*(2), 129–149, 1987.

McLaughlin, D. B., A distributed parameter state space approach for evaluating the accuracy of groundwater predictions, Ph.D. thesis, 206 pp., Princeton Univ., Princeton, N. J., 1985.

McLaughlin, D. B., and W. K. Johnson, Comparison of three groundwater modeling studies, *J. Water Resour. Plann. Mange. Div. Am. Soc. Civ. Eng.*, *113*(3), 405–421, 1987.

McLaughlin, D. B., and E. F. Wood, A distributed parameter approach for evaluating the accuracy of groundwater model predictions, 1, Theory, *Water Resour. Res.*, this issue.

Mizell, S. A., A. L. Gutjahr, and L. W. Gelhar, Stochastic analysis of spatial variability in two-dimensional steady groundwater flow assuming stationary and nonstationary heads, *Water Resour. Res.*, *18*(4), 1053–1067, 1982.

Newland, E., *An Introduction to Random Vibrations and Spectral Analysis*, Longman, New York, 1984.

Pinder, G. F., and W. G. Gray, *Finite Element Simulation in Surface and Subsurface Hydrology*, Academic, San Diego, Calif., 1977.

Sagar, B., Galerkin finite element method for analyzing flow through random media, *Water Resour. Res.*, *14*(6), 1035–1044, 1978.

Smith, L., and R. A. Freeze, Stochastic analysis of steady state groundwater flow in a bounded domain, 1, One-dimensional simulations, *Water Resour. Res.*, *15*(3), 521–528, 1979*a*.

Smith, L., and R. A. Freeze, Stochastic analysis of steady state groundwater flow in a bounded domain, 2, Two-dimensional simulations, *Water Resour. Res.*, *15*(6), 1543–1559, 1979*b*.

Stavroulakis, P. (Ed.), *Distributed Parameter Systems Theory, Part 2, Estimation*, Hutchinson Ross, Stroudsburg, Pa., 1983.

Tang, D. H., and G. F. Pinder, Analysis of mass transport with uncertain physical parameters, *Water Resour. Res.*, *15*(5), 1147–1155, 1979.

Townley, L. R., Numerical models of groundwater flow: Predictions and parameter estimation in the presence of uncertainty, Ph.D. thesis, 335 pp., Mass. Inst. of Technol., Cambridge, 1983.

Yeh, W. W.-G., and Y. S. Yoon, Aquifer parameter estimation with optimum dimension in parameterization, *Water Resour. Res.*, *17*(3), 664–672, 1981.

D. McLaughlin, Room 48-209, Ralph M. Parsons Laboratory, Department of Civil Engineering, Massachusetts Institute of Technology, Cambridge, MA 02139.

E. F. Wood, Water Resources Program, Department of Civil Engineering, Princeton University, Princeton, NJ 08544.

(Received June 6, 1987;
revised March 2, 1988;
accepted March 4, 1988.)